Year: 2021

CT and MRI of a transcardiac gunshot wound with an annular distribution of bullet fragments surrounding an exit-re-entrance wound after the bullet burst from a floor tile upon exiting the lying body

Gascho, Dominic ; Bolliger, Stephan A ; Thali, Michael J

Abstract: This case report describes medicolegal examinations of a decedent with a fatal gunshot wound. The decedent lied on the floor as a bullet was fired into his chest. Computed tomography (CT) and magnetic resonance imaging (MRI) were performed as part of the judicial investigation. The MRI examination was valuable for delineating the wound channel through the left ventricle, which was deemed the main cause for internal bleeding and fatal blood loss. The diagnostic value of CT for the detection of injuries was low in this case. However, CT allowed for the virtual investigation of bullet fragments. According to CT-based dual-energy index calculations, it could be inferred that the fragments were most likely made of lead matching .357 Magnum R–P cartridges that were found at the scene. The bullet fragments were located underneath the skin at the suspected exit wound. The exit wound was actually an exit-re-entrance wound, as it can be assumed that the fragments re-entered the body after the bullet burst from hard ground upon exiting the body of the decedent, who was lying on the floor. CT visualized an uncommon annular distribution pattern for the bullet fragments surrounding the exit-re-entrance wound. The formation of such an annular distribution pattern of bullet fragments and the relevant conclusions that may be drawn from such a distribution pattern are discussed in this article.

DOI: https://doi.org/10.1016/j.jflm.2020.102087

Journal of Forensic and Legal Medicine 77 (2021) 102087

Contents lists available at ScienceDirect

Journal of Forensic and Legal Medicine

journal homepage: http://www.elsevier.com/locate/yjflm

Case report

CT and MRI of a transcardiac gunshot wound with an annular distribution of bullet fragments surrounding an exit-re-entrance wound after the bullet burst from a floor tile upon exiting the lying body

Dominic Gascho *, Stephan A. Bolliger, Michael J. Thali

Department of Forensic Medicine and Imaging, Institute of Forensic Medicine, University of Zurich, Zurich, Switzerland

A R T I C L E I N F O

Keywords:
Bullet
Gunshot
Radiologic wound ballistics
Computed tomography
Magnetic resonance imaging
Postmortem
Dual-energy index

A B S T R A C T

This case report describes medicolegal examinations of a decedent with a fatal gunshot wound. The decedent lied on the floor as a bullet was fired into his chest. Computed tomography (CT) and magnetic resonance imaging (MRI) were performed as part of the judicial investigation. The MRI examination was valuable for delineating the wound channel through the left ventricle, which was deemed the main cause for internal bleeding and fatal blood loss. The diagnostic value of CT for the detection of injuries was low in this case. However, CT allowed for the virtual investigation of bullet fragments. According to CT-based dual-energy index calculations, it could be inferred that the fragments were most likely made of lead matching .357 Magnum R–P cartridges that were found at the scene. The bullet fragments were located underneath the skin at the suspected exit wound. The exit wound was actually an exit-re-entrance wound, as it can be assumed that the fragments re-entered the body after the bullet burst from hard ground upon exiting the body of the decedent, who was lying on the floor. CT visualized an uncommon annular distribution pattern for the bullet fragments surrounding the exit-re-entrance wound. The formation of such an annular distribution pattern of bullet fragments and the relevant conclusions that may be drawn from such a distribution pattern are discussed in this article.

1. Introduction

Postmortem computed tomography (CT) is an accepted method in forensic medicine, and CT scanning is recommended in cases of gunshot wounds.[1] Several studies have highlighted the advantage of postmortem CT in cases involving craniocerebral gunshot wounds. The bullet path is indicated via the detection of blood, air, bone splinters and internal ricochet points, and the direction of the shot is identified by inwardly and outwardly bevelled fractures and radiating fracture lines (Puppe's rule).[2,3] CT is also well known to effectively highlight radiopaque material and locate lodged bullets or fragments.[4,5] Visual assessments of the shape and calibre of a lodged bullet allow us to classify a bullet in situ.[6–9] If a visual assessment is inconclusive, for instance, due to fragmentation, the calculation of the dual-energy index, which describes the ratio between the CT numbers at two different energy levels, provides information on the metallic components of the bullet.[8,10–13] The distribution of fragments frequently indicates the direction of the shot.[14] In special cases, however, the fragments of a bullet display an uncommon distribution pattern; for instance, a concentric circle of bullet fragments around the entrance wound can occur if a bullet re-enters the body after perforating the hand and striking the phalanges.[15] In the detection of soft-tissue injuries, postmortem CT is less sensitive than other methods, especially in cases with thoracoabdominal gunshot wounds.[1,4] Postmortem magnetic resonance imaging (MRI) is more sensitive than CT for the detection of soft-tissue injuries.[16–18] However, due to the limited access to MRI scanners, experiences using postmortem MRI for thoracic or abdominal gunshot wounds in medicolegal investigations are described in only a few cases.[19,20]

The following case describes CT and MRI findings in a forensic case with a fatal transcardial gunshot injury. The highlight in this case is the visualization of an uncommon distribution pattern of bullet fragments surrounding a wound on the back of the decedent. The formation of this distribution pattern and the conclusions that can be drawn from it are discussed.

* Corresponding author. Department of Forensic Medicine and Imaging, Zurich Institute of Forensic Medicine, University of Zurich, Winterthurerstrasse 190/52, CH-8057, Zurich, Switzerland.
E-mail address: dominic.gascho@irm.uzh.ch (D. Gascho).

https://doi.org/10.1016/j.jflm.2020.102087
Received 7 September 2020; Received in revised form 4 November 2020; Accepted 14 November 2020
Available online 21 November 2020

2. Case report and postmortem imaging

2.1. External examination

After a dull noise, the motionless body of a 63-year-old man was found by his wife in his basement. Resuscitation measures were performed by first aiders and continued by paramedics. Despite attempts at resuscitation, the man was ultimately pronounced dead by the emergency doctor. A revolver was found next to the body, and a small hole was visible in the decedent's chest. Therefore, the police, a forensic doctor, and a prosecutor were summoned to the scene.

The revolver was identified as a Trooper MK III .357 Magnum CTG (Colt's Patent Fire Arms Manufacturing Co, Hartford, Connecticut). The cylinder held five .357 Magnum Remington-Peters (R–P) cartridges and one shell of a .357 Magnum R–P cartridge. Furthermore, a pillow was found next to the body. The pillow displayed a large defect, as if it was torn open, on one side and a small defect on the opposite side. The defects of the pillow suggest that a bullet that had been fired through the pillow while the pillow was held in front of the revolver's barrel.

A roundish soft-tissue defect in the decedent's chest was determined as the entrance wound (Fig. 1a). The entrance wound was located between the sternum and the left nipple. After turning the body to a lateral position, a roundish skin defect with brown coffee powder-like soiling was visible in the middle of the back approximately 30 mm (1.18 in) to the left of the spine. (Fig. 1b). Grey fragments stuck superficially in the wound. One of the grey fragments was removed from the wound and attributed to the bullet matching the shell of the .357 Magnum R–P cartridge in the cylinder. At the point where the skin defect on the back touched the ground, a tile exhibited a roundish defect that matched the shape and size of the skin defect (Fig. 1c). The coffee powder-like soiling and small white fragments were attributed to material from this tile. The body demonstrated sparse livor mortis.

The prosecutor commissioned an analysis of the gunshot residue (not described in detail here) and forensic imaging as triage information for conducting an autopsy.

2.2. Computed tomography

CT scans of the entire body, head, and torso were performed using a 128-slice CT scanner (SOMATOM Definition Flash, Siemens Healthcare, Forchheim, Germany). The scan parameters were 120 kVp; 400 mAs as the reference value for dose modulation; and a pitch of 0.35 for the torso CT.[21] The raw data were reconstructed with a slice thickness of 1 mm and 0.8 mm increments using hard (B60) and soft (B30) kernels.

The CT scan depicted a tissue defect at the entrance wound between the 3rd and 4th ribs on the left and a left haemothorax, and the heart was shifted to the middle of the thorax. The wound channel was not identifiable on CT, although it was assumed that the heart may have been injured either by the bullet that perforated the cardiac muscle (permanent wound channel) or due to shearing, compressing, and stretching during temporary cavitation. The bullet did not cause any bone damage when penetrating the body. At the opposite side of the entrance wound along a cranio-caudal trajectory with a descent angle of approximately 17°, the CT scan revealed numerous fragments that were located underneath the skin distal from the 10th rib. These fragments were annularly distributed with a diameter of approximately 45 mm (1.77 in) around the wound on the back of the decedent (Fig. 2). The fragments were determined to be metallic because of the high radiopacity. Only a single fragment was located beyond these annular distributed fragments in the caudal direction in the muscle tissue approximately 20 mm (0.79 in) deep in the skin.

2.3. Dual-energy index

Two additional scans (scan 1: 120 kVp and 145 mAs; scan 2: 140 kVp and 100 mAs) were performed for the region in which bullet fragments were assumed. Reconstructions were performed on an extended CT scale (ECTS) with a slice thickness of 1.5 mm and a hard kernel (B70). Circular region-of-interest (ROI) measurements were performed at the edge (ROI size: 0.5 mm^2) of the separated fragment that was located in the caudal direction beyond the annular distributed fragments (Fig. 3). The dual-energy index was calculated from the maximum CT measurement within the ROIs of the two scans, as described in the literature.[8] The mean value of the dual-energy indexes from the maximum CT numbers within the ROIs of three different slices was −0.003 (SD: 0.002).

2.4. Magnetic resonance imaging

An MRI examination of the thorax was performed using a 3 T MRI scanner (Achieva 3.0T TX, Philips Medical System, Best, The Netherlands) and a 16-channel torso coil. The MRI protocol included a transversal T_1-weighted sequence (TR: 694 ms, TE: 6.35 ms), a transversal T_2-weighted sequence (TR: 5422 ms, TE: 60 ms), a coronal T_2-weighted sequence (TR: 5337 ms, TE: 60 ms), and a transversal T_2-weighted spectral-attenuated inversion recovery (SPAIR) sequence (TR: 7045 ms, TE: 60 ms). A slice thickness of 3 mm was selected for each sequence.

The MRI examination delineated the soft-tissue injuries along the bullet path and confirmed the haemothorax. For the T_2-weighted SPAIR sequence, a hyperintense region was highlighted surrounding the entrance wound, which was indicative of tissue injuries (Fig. 4a). A wound channel through the left ventricle (Fig. 4b) and through the dorsal muscles (Fig. 4c) was identified in the MRI results. The annular distribution of fragments, which was highlighted by CT, was barely visible on MRI, and the metallic fragments presented negligible susceptibility artefacts (Fig. 4d).

2.5. Manner and cause of death

The decedent died from a suicidal gunshot wound causing fatal blood

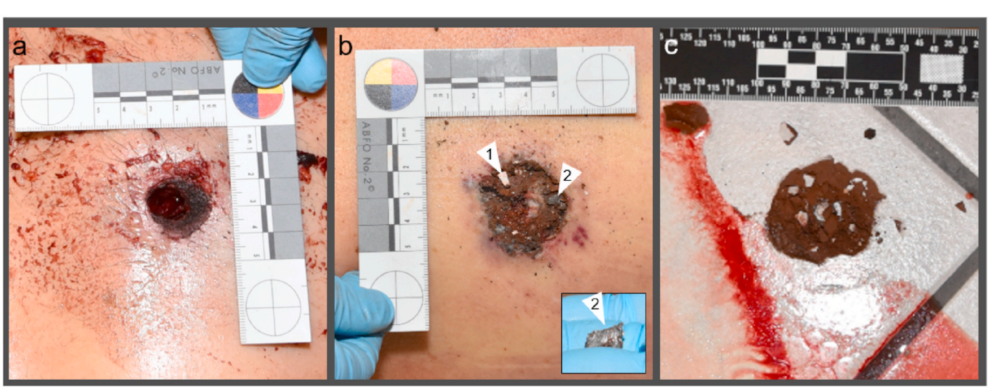

Fig. 1. The entrance wound (a) was located on the left side of the decedent's chest between the sternum and the nipple. A further skin defect (b) was located in the middle of the back slightly left of the spine. White (arrowhead 1) and grey fragments (arrowhead 2) stuck in the wound with brown coffee powder-like soiling are shown. One of the grey fragments was removed from the wound and attributed to a lead bullet. A tile at the point where the skin defect touched the ground displayed a roundish defect (c) matching the size and shape of the skin defect. (For interpretation of the references to colour in this figure legend, the reader is referred to the Web version of this article.)

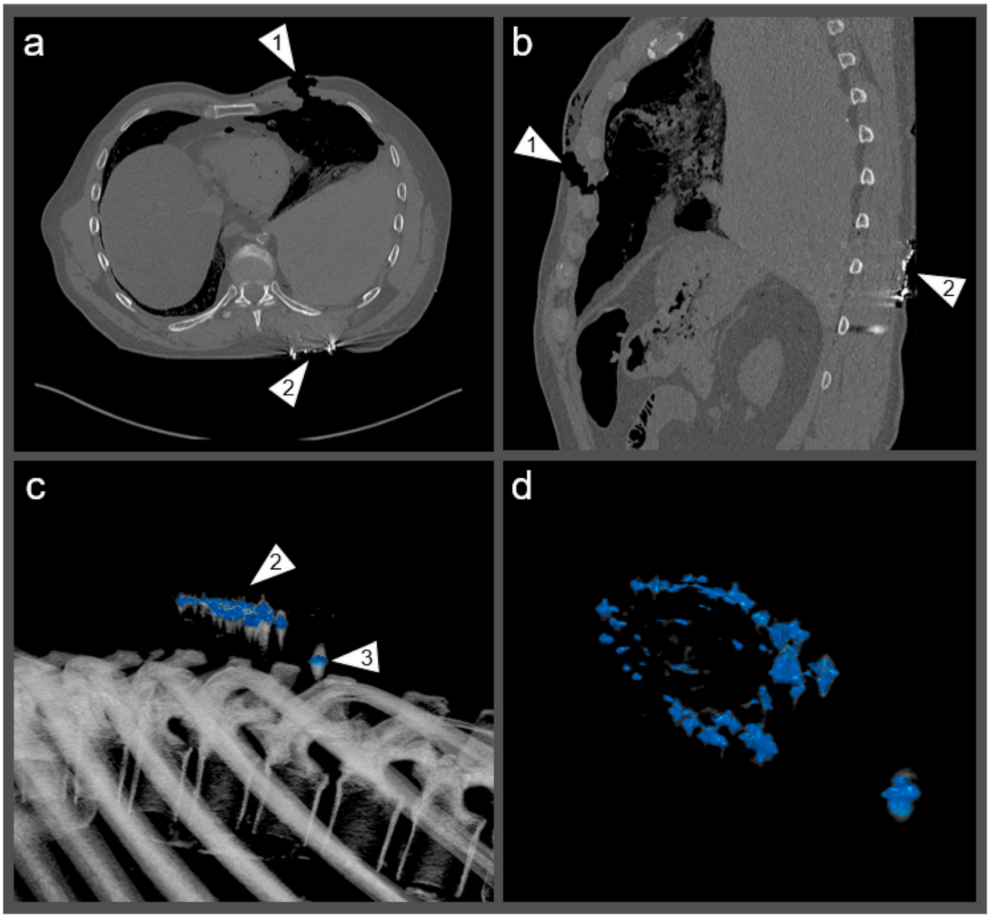

Fig. 2. The entrance wound (arrowhead 1) and numerous bullet fragments located at the skin defect on the back of the decedent (arrowhead 2) were detected in CT-aligned multiplanar reconstructions (a: transversal view; b: sagittal view). Volume renderings (c: sagittal view; d: oblique caudocranial view) revealed an angular distribution pattern for the bullet fragments. A single fragment (arrowhead 3) was located caudal from the other fragments.

loss.

The manner of death was declared suicide because of the results of the rhodizonate staining analysis. Rhodizonate staining analysis revealed an extensive distribution of gunshot residue particles on the left hand of the decedent and few particles on the right hand. The result of the analysis was negative for both hands of the decedent's wife.

The cause of death was deemed internal bleeding and fatal blood loss due to a shot through the heart based on the imaging findings. The wound on the back was defined as an exit-re-entrance wound. The prosecutor waived an additional autopsy.

3. Discussion

The CT examination revealed an annular distribution pattern of bullet fragments directly under the skin surrounding an exit-re-entrance wound. The bullet fragments most likely re-entered the body after the bullet burst by hitting the tile directly underneath the body. Considering the intracorporeal trajectory and the lying position of the body, the bullet hit the tile at an almost vertical angle of 73° (descent angle: 17°), which most likely caused such an annular distribution of the fragments at the exit-re-entrance wound. During the external examination, the exit-re-entrance wound presented soiling, and small fragments of tile were stuck in the wound, which indicated that a hard surface blocked the bullet from exiting the body. However, an external assessment may fail in identifying an exit-re-entrance wound if the body is in a state of decomposition or is badly destroyed after charring.[4] In such cases, the use of CT scanning as a screening method can reveal projectiles in the charred or decomposed body.[22,23] While cone beam CT scans demonstrate relatively fewer metal artefacts, multi-slice CT scans require metal artefact reduction algorithms for the assessment of soft tissue and bones on the cross-section images where the lodged bullets or fragments cause severe streak artefacts.[24–28] For investigating the lodged bullet, in turn, an extension of the standard Hounsfield unit scale using special reconstruction techniques is advantageous.[29] The use of micro-CT for the detection of tiny gunshot residue particles on removed samples can be valuable for differentiating between entrance and exit wounds or even between gunshot and stab wounds, which can be challenging in charred or decomposed bodies.[30,31] With regard to the present case, the location of fragments at an exit-re-entrance wound may indicate that the body was lying on hard ground or leaning against a wall when the shot was fired, while an annular distribution pattern in combination with the intracorporeal trajectory may provide a clue on the impact angle. It is conceivable that a very flat impact angle will rather not create an annular distribution for fragments. An annular distribution pattern for the bullet fragments may be of particular value in cases in which the decedent is found somewhere other than the crime scene.

The dual-energy index of the separated fragment was in accordance with that for lead bullets.[8,11,13] The dual-energy index provides a material-based classification metric for a lodged bullet or bullet fragments in situ, but for thorough ballistic analysis, the bullet or fragment has to be recovered from the body. Thus, the calculation of a dual-energy index for the classification of bullets or fragments plays a marginal role in postmortem investigations. For living gunshot victims, however, CT-based material differentiation may be of particular interest if a bullet or fragment cannot be recovered from the patient.[29]

In the present case, the manner of death was determined as suicide

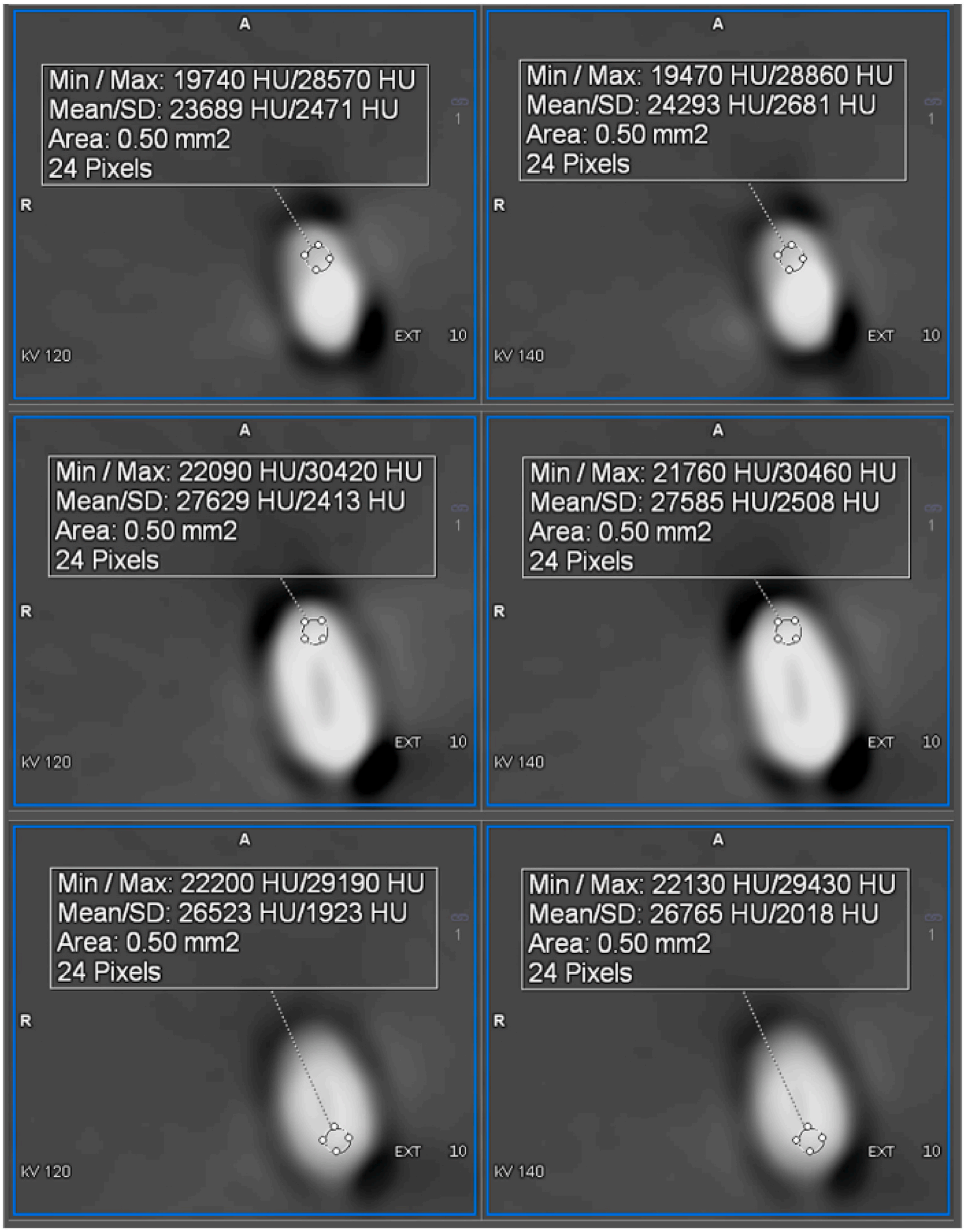

Fig. 3. The mean value of the DEIs from maximum CT numbers within ROIs in three different slices of the images obtained with 120 kVp (left column) and 140 kVp (right column) was −0.003 (SD: 0.002). The DEIs are consistent with those from lead bullets, which supports the visual assessment of the removed fragments during the external examination.

according to the results of the rhodizonate staining analysis, the cause of death was determined from the imaging findings, and an additional autopsy was waived. The authors of recent articles[1,32] have considered CT in combination with an external examination suitable for triaging decedents with gunshot wounds, in which case an autopsy can be waived; alternatively, targeted dissection (together with toxicology) can be performed to supersede a full autopsy. However, postmortem CT has a low sensitivity for the detection of cardiac injuries in firearm death.[1] This limitation is evident in the present case, as only the MRI result allowed for a reliable diagnosis of the cause of death, namely, the injured heart leading to internal bleeding and fatal blood loss. Although MRI is more sensitive to soft-tissue injuries than CT, this imaging modality is still considered less accurate for the identification of the cause of death and is usually only considered for the diagnosis of natural deaths related to diseases of the cardiovascular or central nervous system.[33,34] However, this valuation refers to the fact that only a few studies have evaluated the use of postmortem MRI for medicolegal purposes to date. The diagnostic opportunities using dedicated MRI sequences for specific forensic questions have not been fully explored. The limited access to MRI scanners for postmortem examinations, the complexity of the imaging technology, and the complex image review process are certainly major factors related to this limitation.

In conclusion, the distribution pattern of bullet fragments in combination with the wound channel may provide clues to the location of the scene and to the position of the body when the shot was fired. A rough classification of the metallic components of the fragments is feasible without removing them from the body. With regard to the detection of cardiac injuries in cases of transcardiac gunshot wounds, an MRI examination is preferable and may be a valuable addition to CT, especially if an autopsy is waived.

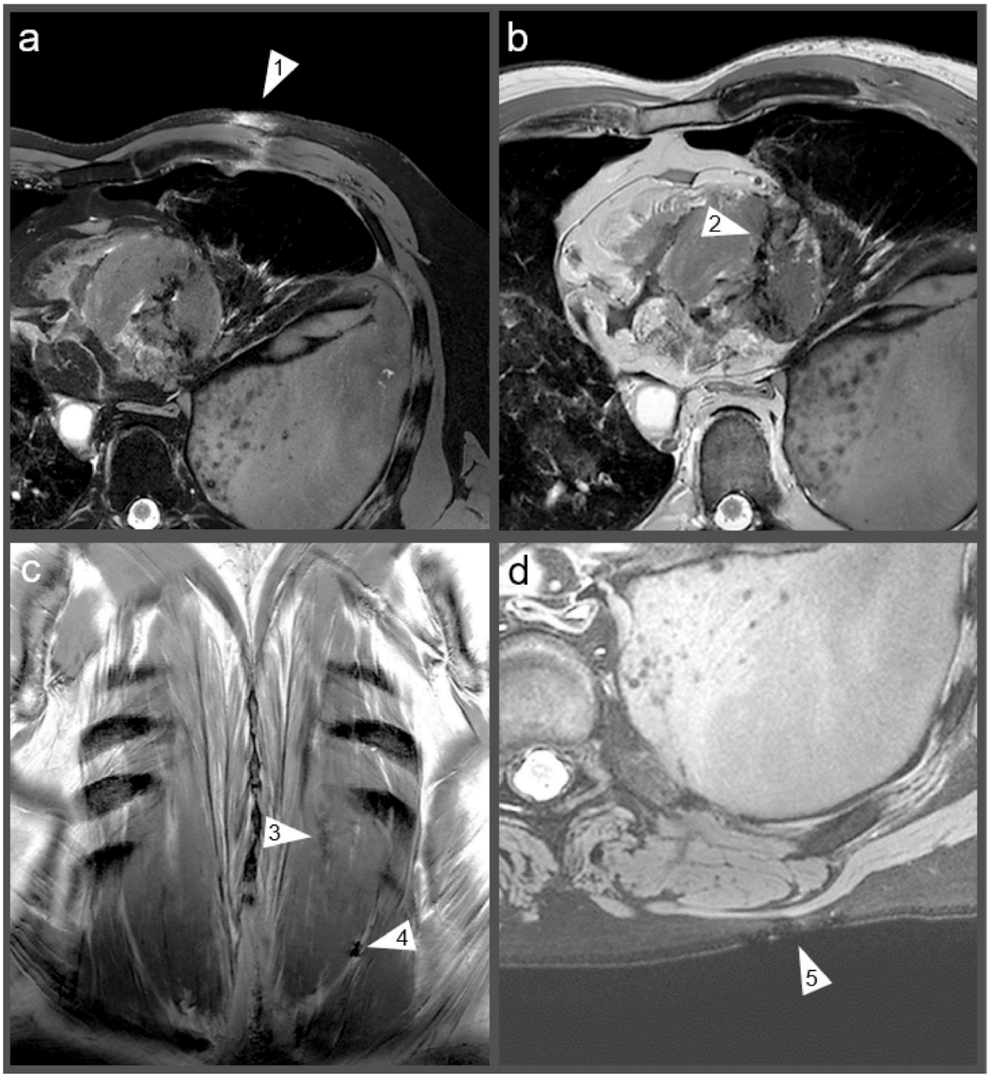

Fig. 4. Soft-tissue injuries were delineated based on a postmortem MRI (a: transversal T_2-weighted SPAIR sequence; b: transversal T_2-weighted sequence; c: coronal T_2-weighted sequence; d: transversal T_2-weighted sequence with a high window level). The MRI findings indicated a T_2-hyperintense region surrounding the entrance wound (arrowhead 1), a wound channel through the left ventricle (arrowhead 2), and a wound channel through the dorsal muscles (arrowhead 3). The bullet fragments (arrowhead 4: single bullet fragment; arrowhead 5: annular distributed bullet fragments) were hardly identifiable in the MRI result since few susceptibility artefacts were detected, which indicated the absence of any ferromagnetic components.

Funding

This scientific paper received no external funding.

Compliance with ethical standards

Ethical approval was waived by the responsible ethics committee of the Canton of Zurich (*waiver number: 2015–0686*). This article does not contain any studies with (living) human participants.

Declaration of competing interest

None of the authors has a real or perceived conflict of interest in any of the material that is presented in the manuscript. The authors have no conflicts of interest to report.

Acknowledgments

The authors express their gratitude to Emma Louise Kessler for her donation to the Zurich Institute of Forensic Medicine, University of Zurich, Switzerland.

References

1. Vester MEM, Nolte KB, Hatch GM, Gerrard CY, Stoel RD, van Rijn RR. Postmortem Computed Tomography in Firearm Homicides: A Retrospective Case Series. *J. Forensic Sci.* 2020;65:1568–1573. https://doi.org/10.1111/1556-4029.14453.
2. Giorgetti A, Giraudo C, Viero A, et al. Radiological investigation of gunshot wounds: a systematic review of published evidence. *Int J Leg Med.* 2019;133:1149–1158. https://doi.org/10.1007/s00414-019-02071-8.
3. Viel G, Gehl A, Sperhake JP. Intersecting fractures of the skull and gunshot wounds. Case report and literature review. *Forensic Sci Med Pathol.* 2009;5:22–27. https://doi.org/10.1007/s12024-008-9062-8.
4. Andenmatten MA, Thali MJ, Kneubuehl BP, et al. Gunshot injuries detected by post-mortem multislice computed tomography (MSCT): a feasibility study. *Leg Med.* 2008;10:287–292. https://doi.org/10.1016/j.legalmed.2008.03.005.
5. Maiese A, Gitto L, De Matteis A, Panebianco V, Bolino G. Post mortem computed tomography: useful or unnecessary in gunshot wounds deaths? Two case reports. *Leg Med.* 2014;16:357–363. https://doi.org/10.1016/j.legalmed.2014.06.005.
6. Marais AAS, Dicks HJ. Utilization of X-ray computed tomography for the exclusion of a specific caliber and bullet type in a living shooting victim. *J Forensic Sci.* 2019; 64:264–269. https://doi.org/10.1111/1556-4029.13805.
7. Alves AM, Picoli FF, Silveira RJ, et al. When forensic radiology meets ballistics–in vivo bullet profiling with computed tomography and autopsy validation: a case report. *Forensic Imaging.* 2020;20:200357. https://doi.org/10.1016/j.fri.2020.200357.
8. Gascho D, Zoelch N, Deininger-Czermak E, et al. Visualization and material-based differentiation of lodged projectiles by extended CT scale and the dual-energy index. *J. Forensic Leg. Med.* 2020;70:101919. https://doi.org/10.1016/j.jflm.2020.101919.
9. Gascho D, Zoelch N, Deininger-Czermak E, et al. In situ identification of Action 4, SECA and QD-PEP bullets from special police ammunitions by computed tomography. *Med Sci Law.* 2020, 0025802420911555. https://doi.org/10.1177/0025802420911555.

10. Diallo I, Auffret M, Deloire L, Saccardy C, Aho S, Ben Salem D. Is dual-energy computed tomography helpful to determinate the ferromagnetic property of bullets? *J. Forensic Radiol. Imaging.* 2018;15:21–25. https://doi.org/10.1016/j.jofri.2018.10.001.
11. Gascho D, Zoelch N, Richter H, Buehlmann A, Wyss P, Schaerli S. Identification of bullets based on their metallic components and X-ray attenuation characteristics at different energy levels on CT. *Am J Roentgenol.* 2019;213:W105–W113. https://doi.org/10.2214/AJR.19.21229.
12. Ognard J, Dissaux B, Diallo I, Attar L, Saccardy C, Salem DB. Manual and fully automated segmentation to determine the ferromagnetic status of bullets using computed tomography dual-energy index: a phantom study. *J Comput Assist Tomogr.* 2019;43:799–804. https://doi.org/10.1097/RCT.0000000000000899.
13. Gascho D, Zoelch N, Richter H, et al. Heavy metal in radiology: how to reliably differentiate between lodged copper and lead bullets using CT numbers. *Eur. Radiol. Exp.* 2020;4:43. https://doi.org/10.1186/s41747-020-00168-z.
14. Harcke HT, Levy AD, Getz JM, Robinson SR. MDCT analysis of projectile injury in forensic investigation. *Am J Roentgenol.* 2008;190:W106–W111. https://doi.org/10.2214/AJR.07.2754.
15. Thali MJ, Kneubuehl BP, Dirnhofer R, Zollinger U. Body models in forensic ballistics: reconstruction of a gunshot injury to the chest by bullet fragmentation after shooting through a finger. *Forensic Sci Int.* 2001;123:54–57. https://doi.org/10.1016/S0379-0738(01)00519-9.
16. Thali MJ, Yen K, Vock P, et al. Image-guided virtual autopsy findings of gunshot victims performed with multi-slice computed tomography (MSCT) and magnetic resonance imaging (MRI) and subsequent correlation between radiology and autopsy findings. *Forensic Sci Int.* 2003;138:8–16. https://doi.org/10.1016/S0379-0738(03)00225-1.
17. Gascho D, Tappero C, Zoelch N, et al. Synergy of CT and MRI in detecting trajectories of lodged bullets in decedents and potential hazards concerning the heating and movement of bullets during MRI. *Forensic Sci Med Pathol.* 2019:1–12. https://doi.org/10.1007/s12024-019-00199-y.
18. Gascho D, Marosi M, Thali MJ, Deininger-Czermak E. Postmortem Computed Tomography and Magnetic Resonance Imaging of Gunshot Wounds to the Neck. *J. Forensic Sci.*. 2020:1360–1364 https://doi.org/10.1111/1556-4029.14311.
19. Heimer J, Gascho D, Odermatt R, et al. Full virtual autopsy in a case of a suicidal transthoracic gunshot injury, Forensic Imaging, 200368 https://doi.org/10.1016/j.fri.2020.200368; 2020.
20. Gascho D, Bolliger SA, Thali MJ, Tappero C. Postmortem computed tomography and magnetic resonance imaging of an abdominal gunshot wound. *Am J Forensic Med Pathol.* 2020;41:119–123. https://doi.org/10.1097/PAF.0000000000000547.
21. Gascho D, Thali MJ, Niemann T. Post-mortem computed tomography: technical principles and recommended parameter settings for high-resolution imaging. *Med Sci Law.* 2018;58:70–82. https://doi.org/10.1177/0025802417747167.
22. Sano R, Hirawasa S, Kobayashi S, et al. Use of postmortem computed tomography to reveal an intraoral gunshot injuries in a charred body. *Leg Med.* 2011;13:286–288. https://doi.org/10.1016/j.legalmed.2011.07.004.
23. Gascho D, Thali MJ, Bolliger SA. Hidden shot pellets on postmortem computed tomography and their utilization for radiologic identification of decedents. *Forensic Sci Med Pathol.* 2020;16:340–344. https://doi.org/10.1007/s12024-019-00213-3.
24. Stuehmer C, Essig H, Bormann K-H, Majdani O, Gellrich N-C, Rücker M. Cone beam CT imaging of airgun injuries to the craniomaxillofacial region. *Int J Oral Maxillofac Surg.* 2008;37:903–906. https://doi.org/10.1016/j.ijom.2008.07.007.
25. Stuehmer C, Blum KS, Kokemueller H, et al. Influence of different types of guns, projectiles, and propellants on patterns of injury to the viscerocranium. *J Oral Maxillofac Surg.* 2009;67:775–781. https://doi.org/10.1016/j.joms.2008.08.036.
26. von See C, Bormann K-H, Schumann P, Goetz F, Gellrich N-C, Rücker M. Forensic imaging of projectiles using cone-beam computed tomography. *Forensic Sci Int.* 2009;190:38–41. https://doi.org/10.1016/j.forsciint.2009.05.009.
27. Berger F, Niemann T, Kubik-Huch RA, Richter H, Thali MJ, Gascho D. Retained bullets in the head on computed tomography – get the most out of iterative metal artifact reduction. *Eur J Radiol.* 2018;103:124–130. https://doi.org/10.1016/j.ejrad.2018.04.019.
28. Douis N, Formery AS, Hossu G, et al. Metal artifact reduction for intracranial projectiles on post mortem computed tomography. *Diagn. Interv. Imaging.* 2020;101:177–185. https://doi.org/10.1016/j.diii.2019.10.009.
29. Gascho D. Lodged bullets on computed tomography: three classification procedures for the virtual investigation of bullets or their fragments that cannot be recovered from the living patient. *Med Sci Law.* 2020;60:245–248. https://doi.org/10.1177/0025802420962697.
30. Fais P, Giraudo C, Boscolo-Berto R, et al. Micro-CT features of intermediate gunshot wounds severely damaged by fire. *Int J Leg Med.* 2013;127:419–425. https://doi.org/10.1007/s00414-012-0775-6.
31. Cecchetto G, Amagliani A, Giraudo C, et al. MicroCT detection of gunshot residue in fresh and decomposed firearm wounds. *Int J Leg Med.* 2012;126:377–383. https://doi.org/10.1007/s00414-011-0648-4.
32. Herath JC, Herath SO. Is it time for targeted and minimally invasive post-mortem examination using total body computed tomography in a medicolegal autopsy? *Forensic Sci Med Pathol.* 2020. https://doi.org/10.1007/s12024-020-00279-4.
33. Roberts IS, Benamore RE, Benbow EW, et al. Post-mortem imaging as an alternative to autopsy in the diagnosis of adult deaths: a validation study. *Lancet.* 2012;379:136–142. https://doi.org/10.1016/S0140-6736(11)61483-9.
34. Cartocci G, Santurro A, Frati P, Guglielmi G, La Russa R, Fineschi V. Imaging techniques for postmortem forensic radiology. In: Lo Re G, Argo A, Midiri M, Cattaneo C, eds. *Radiol. Forensic Med. Identif. Post-Mortem Imaging.* Cham: Springer International Publishing; 2020:29–42. https://doi.org/10.1007/978-3-319-96737-0_5.